PROCEEDINGS of the
23rd International Congress on Acoustics

9 to 13 September 2019 in Aachen, Germany

Aeroacoustic simulation and experimental validation of sound emission of an axial fan applied in a heat pump

Andreas LUCIUS[1]; Marc SCHNEIDER[1]; Stefan SCHWEITZER-DE BORTOLI[2], Tom GERHARD[3], Thomas GEYER[4]

[1] ebm-papst Mulfingen, Germany

[2] Vaillant, Germany

[3] former Vaillant, Germay

[4] Brandenburg Universtity of Technology, Germany

ABSTRACT

The reduction of noise emission of heat pumps is a major development target for the appliance manufacturer. An important source of sound is the fan. The fan is operating at disturbed inflow conditions due to installation in the appliance. Additionally small scale turbulence generated by the heat exchanger further increases fan noise emission. Noise emission may be reduced via improved installation or specific fan design. The aim of the project was to measure flow and turbulence characteristics inside the heat pump via constant temperature anemometry as well as noise emission. The acquired data set was then used for validation of CFD and CAA simulations. The effect of inflow turbulence was analyzed for configurations with and without heat exchanger. Hot wire measurements show increased average turbulence levels of 20 percent downstream the heat exchanger. In a second step URANS simulations were conducted for both configurations. The heat exchanger was modelled as porous medium. Turbulence properties could be matched with experiments with reasonable boundary conditions at the heat exchangers outlet. There is some deviation in flow rate with URANS. Increased tonal noise for the configuration with heat exchanger is predicted but the levels are in error of up to 10 dB.

Keywords: fan noise, heat pump, turbulence, CAA

1. INTRODUCTION

The reduction of CO_2 emissions is one of the most important global challenges. In Germany conventional heating with gas or oil dominates the installed heating systems. An alternative to the usage of fossil fuels for heating are heat pumps. These machines use electrical power to transfer environmental heat to useable heat. If the electrical power is generated from renewable sources the operation is CO_2 neutral. The increasing number of installed heat pumps in human environment like gardens raises the importance of noise emissions. The axial fan is one of the key components of a heat pump. In addition to the compressor the fan is the most important source of noise. This paper analyzes the influence of the heat exchanger as turbulence generator on fan noise emission. The heat exchanger is expected to generate small scale turbulence. On the other hand it acts as a flow straightener. Large scale vortical structures are broken and flow homogeneity is increased. The present paper analyzes the influence of the heat exchanger on fan noise emission as well as its influence on turbulent inflow conditions.

Disturbed turbulent inflow conditions are well known to increase fan noise (1). Turbulent ingestion noise on airfoils has been the topic of numerous research papers in the past. Recent studies on increased fan noise due to inflow disturbance are e.g. the work of Zenger et. al. (2). The influence of the heat exchanger in an automotive cooling fan was analyzed by Rynell et. al. (3). He found, that removing the heat exchanger in his setup increases fan noise. This is in line with the work of Lucius et al. (4), who showed dramatic increase for a rectangular box as inflow disturbance. The heat exchanger

[1] Andreas.Lucius@de.ebmpapst.com

itself generates small scale turbulence due to flow separation at the cooling tubes. But additionally the narrow lamellas act as a flow straightener. Large scale turbulent structures as corner vortices from the box are broken by the heat exchanger. The aim of the current study is to analyze the effect of inflow turbulence on fan noise in a heat pump. There is only limited knowledge of turbulence properties of the flow after a heat exchanger. Length scales and turbulence intensity are the key parameters that determine the leading edge noise. The work of Czwielong et. al. (5) shows hot wire measurements after different heat exchanger configurations. These measurements were done without fan at the leading position. The measurements show high turbulence intensity and anisotropy. The flow is accelerated from rectangular heat exchanger cross section to the fan housing, which leads to vortex stretching and the high level of anisotropy reported.

In the present paper hot wire measurements were done inside a heat pump. Two configurations were analyzed: The base configuration and a second setup without heat exchanger. Configurations are displayed in Figure 1.

Figure 1. Configurations analyzed, left base configuration, right without heat exchanger (HEX)

2. Experimental results

2.1 Experimental setup and acoustic results

In order to analyze the effect of inflow turbulence due to the heat exchanger the two configurations were measured in different test rigs. First of all acoustic and aerodynamic performance was measured in a test rig according to DIN EN ISO 5801. The test rig is an anechoic room with reflecting bottom. Pressure side and suction side are separated with a wall. The heat pump is mounted at the chamber wall. Tape was used to prevent any airflow leakage between inlet and outlet of the heat pump. The heat pump was lifted from the bottom such that fan axis is 1.5 m above the reflecting bottom. Additional throttling was applied to see the influence of the operational point on the acoustic performance. Sound power was measured on suction and pressure side with the enveloping surface method. Results shown in this paper are focused on inlet sound power. Figure 2 shows the suction side overall sound power for the two configurations. The configuration with heat exchanger (HEX) shows up to 1 dB higher sound power. This is not in line with the results of Rynell et al. (3). The main reason for this behavior is attributed to the asymmetric disturbed inflow conditions even with the heat exchanger installed (see Figure 5). The inverter marked in blue is a very narrow disturbance, which has probably more effect than flow separation from the casing if the heat exchanger is removed.

There is some dependence of overall sound power on flow rate with steep increase at low flow rates. The fan installed in the heat pump with heat exchanger operates near the point of minimal noise emission. The additional pressure loss of the heat exchanger results in a reduction of flow rate of 18 % at free blowing conditions.

Sound power 3rd octave spectra are shown in the right hand side of Figure 2. Both configurations are displayed at the reference flow rate of the base configuration. For the configuration without heat exchanger the sound spectrum at free blowing conditions is additionally shown. At the same flow rate there is an increase of broad band noise of 1 to 2 dB for frequencies up to 2 kHz in case of heat exchanger installed. At higher frequencies acoustic damping of the heat exchanger reduces inlet sound power. With increased flow rate noise emission at nearly all frequencies is 1 to 2 dB higher.

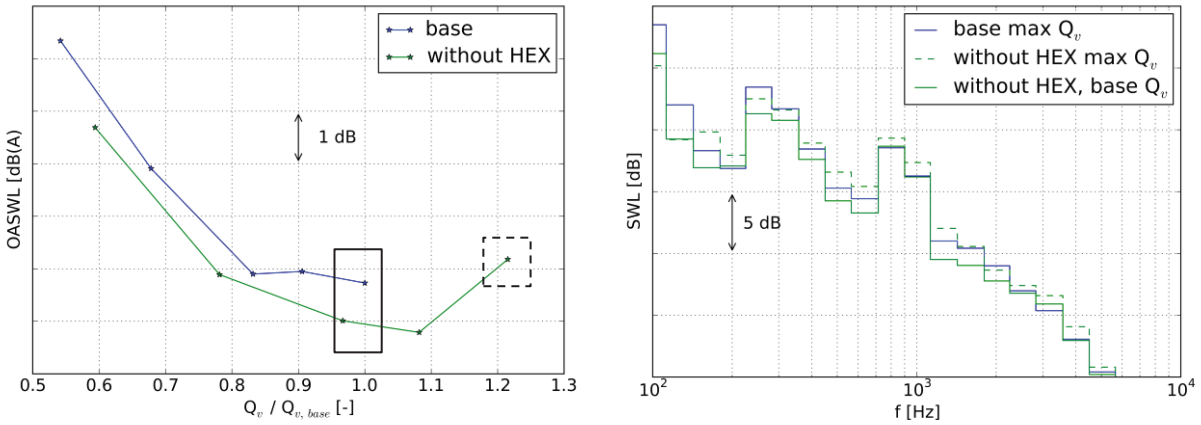

Figure 2. Overall sound power performance curve and 3rd octave spectra

2.2 Detailed measurements of flow velocity

Flow velocity inside the heat pump was measured with Constant Temperature Anemometry (CTA). The measurements were conducted outside the performance test rig. In this measurement setup it was not possible to measure or control the air flow rate. Flow rate is different for both configurations as shown in section 2.1. A DANTEC 55P64 probe was applied to measure flow in fan axial direction and vertical direction according to Figure 1. The probe was mounted on a 2D automatic traverse system. Velocity was measured for 12 s in each point, first 2 seconds are skipped in evaluation due to potential probe vibration after traversing. The sampling frequency was 25.6 kHz, spectra are generated from blocks with 16384 points. A rectangular grid of 6 x 6 points with a spacing of 40 mm covers little more than one quadrant of the fan circumference. The installation is asymmetric mainly due to the inverter box (see Figure 5). All measurements consider the air flow path only, the cooling circuit was not in operation. The fan installed is a 3 bladed axial fan of 450 mm diameter. The fan is directly mounted on the EC motor running at 620 revolutions per minute.

Two measurement planes at different distances to the fan are measured to get an impression on turbulent dissipation. The measurement planes are located at 40 and 80 mm downstream the heat exchanger. All diagrams in this paper concerning detailed flow analysis refer to the 80 mm position. The axial distance between fan leading edge and heat exchanger is 158 mm. A comparison of measured axial velocities is shown in Figure 3. As expected flow velocities are higher for the configuration without heat exchanger. However the difference is higher than 21 % expected from flowrate. The flow field is more homogeneous for the base configuration. This is especially true for the border points. In addition there is a radial distribution with low velocity region near the impeller hub for configuration 2. Turbulence intensities for both configurations are shown in the lower part of Figure 3. The turbulence intensity displayed is normalized with the local mean axial velocity. The heat exchanger leads to a virtual increase of turbulence levels from near zero to 17% in the core region. Near the borders turbulence levels are higher for the configuration without heat exchanger. This is attributed to flow separation from the casing. This can have dramatic influence on fan acoustics (4). Velocity fluctuations are quite similar for both measured directions, so only the axial velocity is shown in this paper.

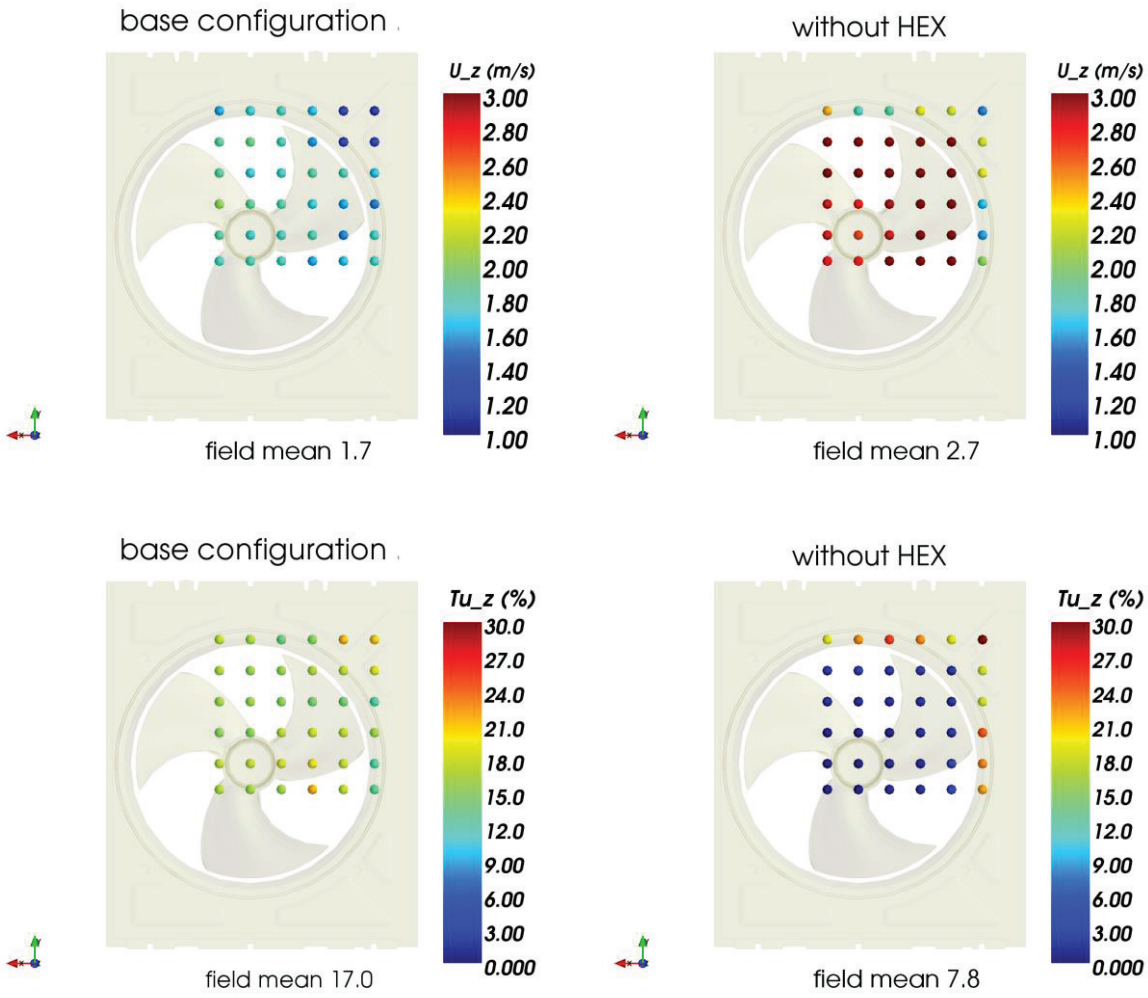

Figure 3. Measured axial velocity (top) and turbulence intensity (bottom) for both configurations

The influence of the heat exchanger on turbulent spectra is shown in Figure 4. The curve shows velocity spectra of the axial velocity for all measured points 80 mm downstream the heat exchanger. For the base configuration all spectra coincide within a narrow band. There are two tonal components in the spectrum. One peak is at 33 Hz which is the blade passing frequency. The other peak at 56 Hz corresponds to vortex shedding at the heat exchanger tubes. This peak corresponds to a Strouhal number of 0.23 with mean axial flow velocity and tube diameter as length scale. Configuration 2 without heat exchanger shows quite different behavior. There are some points with very low fluctuations, these points are located near the rotation axis. The other group of points contains large amount of kinetic energy especially at low frequencies. These are probes located close to the boundary edges. In addition to kinetic energy, turbulent length scales are evaluated from the autocorrelation of velocity fluctuations. Measured and simulated length scales are discussed in section 3.2.

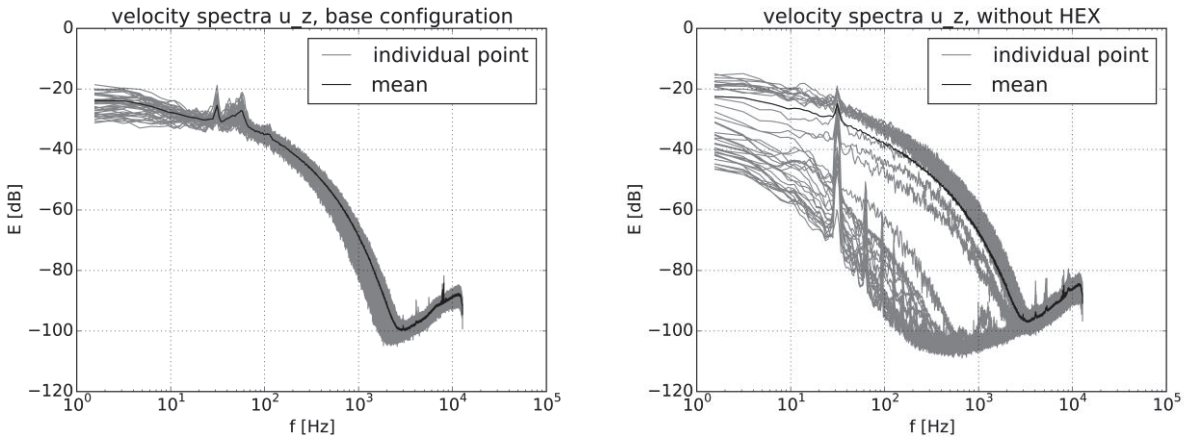

Figure 4. Measured turbulent velocity spectra for both configurations

3. CFD setup and results

3.1 URANS simulations

CFD simulations were conducted with the general purpose CFD code STAR-CCM+ 12.06. The k-ε realizable turbulence model was chosen. All simulations were done with compressible air, as the acoustics is taken into account. The boundary conditions are chosen to obtain the free blowing operating point (zero pressure outlet and stagnation inlet). For the transient simulations non-reflecting boundary conditions were applied. Suction side and pressure side are separated in the modelled geometry as shown in Figure 5. The heat exchanger is modelled as a porous medium (displayed in yellow). All simulations start with a stationary Multi-Reference-Frame simulation with frozen rotor position. These simulations lead to large underestimation of flow rate in range of 30 %. Agreement with measurements is much better if transient fan rotation is included. Temporal resolution is 100 steps per pitch with a second order discretization scheme. Total number of cells for the URANS computation is 19 million polyhedrals. The mesh is identical for both configurations. The boundary layer is resolved with 12 prism layers on the fan blade and on the cylindrical part of the casing. Integral values show negligible differences between a coarser mesh containing 13 million cells. The aeroacoustic pressure is determined with the FW-H solver of STAR-CCM+. The far field sound pressure at 2 microphone locations on the suction side is calculated propagating from a permeable emission surface displayed in green in Figure 5.

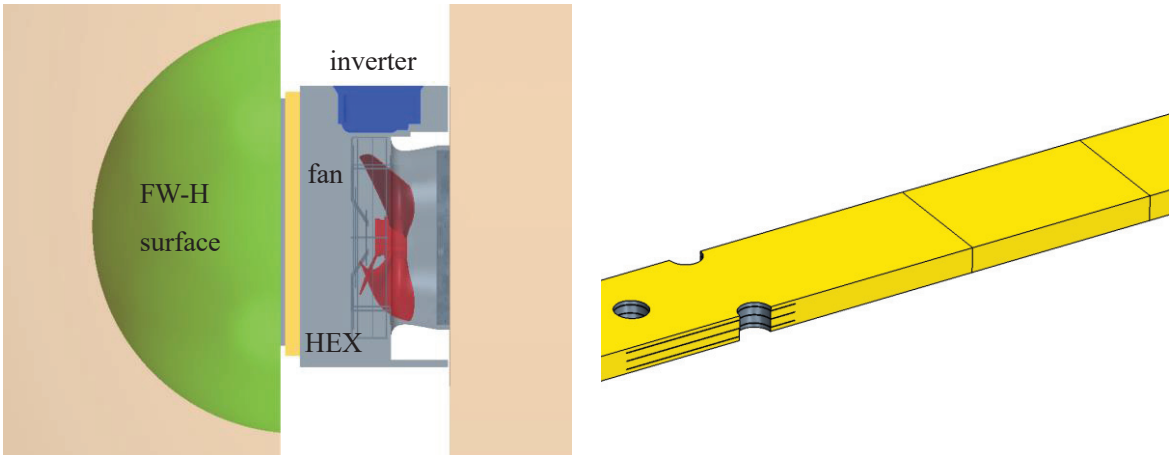

Figure 5. CFD simulation models, left heat pump, right periodic HEX model

3.2 Heat exchanger calibration

The heat exchanger was modelled as a porous medium. For calibration of the model coefficients a periodic model of the detailed heat exchanger geometry (tubes and lamellas) was simulated. Figure 5 shows the simulated geometry. Cooling lamellas were simplified as flat plates. These simulations were used to check pressure loss depending on flow rate and turbulence properties downstream the heat exchangers. The simulations were run unsteady due to vortex shedding at the cooling tubes. A stable solution from steady state RANS could not be achieved.

The obtained pressure loss of 9 Pa is 30 % lower compared to the pressure rise of the fan alone at the same operating point. This is attributed to the simplified geometry. For the momentum equations in the porous region only the inertial term was used. Pressure loss coefficient was set according to fan pressure rise. Turbulence intensity Tu and length scale Λ are evaluated from the CFD with the assumption of isotropic turbulence. In equation (1) U_z is the axial velocity and k the turbulent kinetic energy. The length scale is evaluated from kinetic energy and dissipation rate ε.

$$Tu = \frac{\sqrt{\frac{2}{3}k}}{|U_z|} \tag{1}$$

$$\Lambda = 0.54\frac{k^{3/2}}{\epsilon} \tag{2}$$

Figure 6 shows the averaged CFD results in comparison to the correlation of Roach (6) for parallel rods with the tube diameter D of 7 mm used as length. Correlation and simulation results for the periodic model coincide quite well. For turbulence intensity there is some difference at small distances where the correlation is not valid. The graphs also show the average measured value of turbulent length scale and turbulence intensity for both measurement planes. These values correspond quite well to CFD and Roach correlation. The experiments indicate higher turbulent length scales than expected at the shorter distance. This may be attributed to the short distance to the heat exchanger which is below the data limit of 10 D in (6). As shown in section 2.2 measured kinetic energy also contains contribution due to impeller rotation. This content is not broad and for that reason is not included in the modelled kinetic energy. For that reason measured kinetic energy is expected to be higher than from CFD results. CFD data of the periodic model will now be used as input for the porous medium in the full simulation. Fitting turbulence is quite challenging. The boundary conditions in terms of length scale and turbulence intensity are specified at heat exchanger outlet. Turbulence intensity dissipates with distance depending on the length scale applied. Initial RANS simulations of decaying turbulence from turbulent inflow conditions were performed. It was not possible to fit both properties (Λ and Tu) at measured locations. RANS with turbulent inlet boundary lead to a decay similar to Roach, which has stronger dissipation compared to the periodic resolved HEX model. A variation of inlet parameters was done in order to fit turbulence intensity. The best fit was achieved with considerable larger length scales. The chosen turbulent properties at HEX outlet are Tu = 30 % and Λ = 4.5 mm. These values are used as input for the full simulation of the base configuration with heat exchanger.

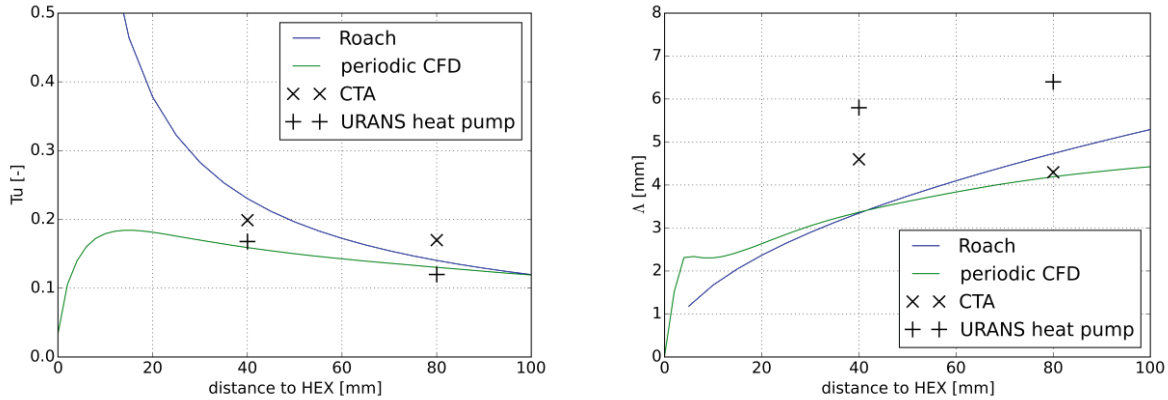

Figure 6. Turbulence properties from experiments and simulations

3.3 URANS Results

In this section URANS simulation results are discussed. The results correspond to temporal mean values averaged over 5 out of 8 rotor revolutions. Table 1 shows integral performance in comparison to measured values. Absolute flow rate Q_v is ca. 10% smaller compared to the experiments for both configuration, but the increase of 21 % in flow rate between configuration 1 and 2 is well predicted. Simulated velocity and turbulence fields are shown in Figure 7. Velocities are quite well predicted for both configurations. However there is an offset due to error in flow rate. In addition flow field is more homogeneous in simulations compared to measured results. With proper settings for the porous medium good agreement of turbulence levels is achieved (see Figure 6). Simulations show flow separation from the casing for configuration 2. Velocity defects and high levels of turbulence similar to measurements are found in the outer region of the measurement planes.

Table 1. URANS results vs experiments

configuration	nr. of cells	CFD	experiment
		Q_v / Q_v Base Exp.	Q_v / Q_v Base Exp.
1	$1.9\ 10^7$	0.889	1.0
2	$1.9\ 10^7$	1.066 (+19.7%)	1.215 (+21.5%)

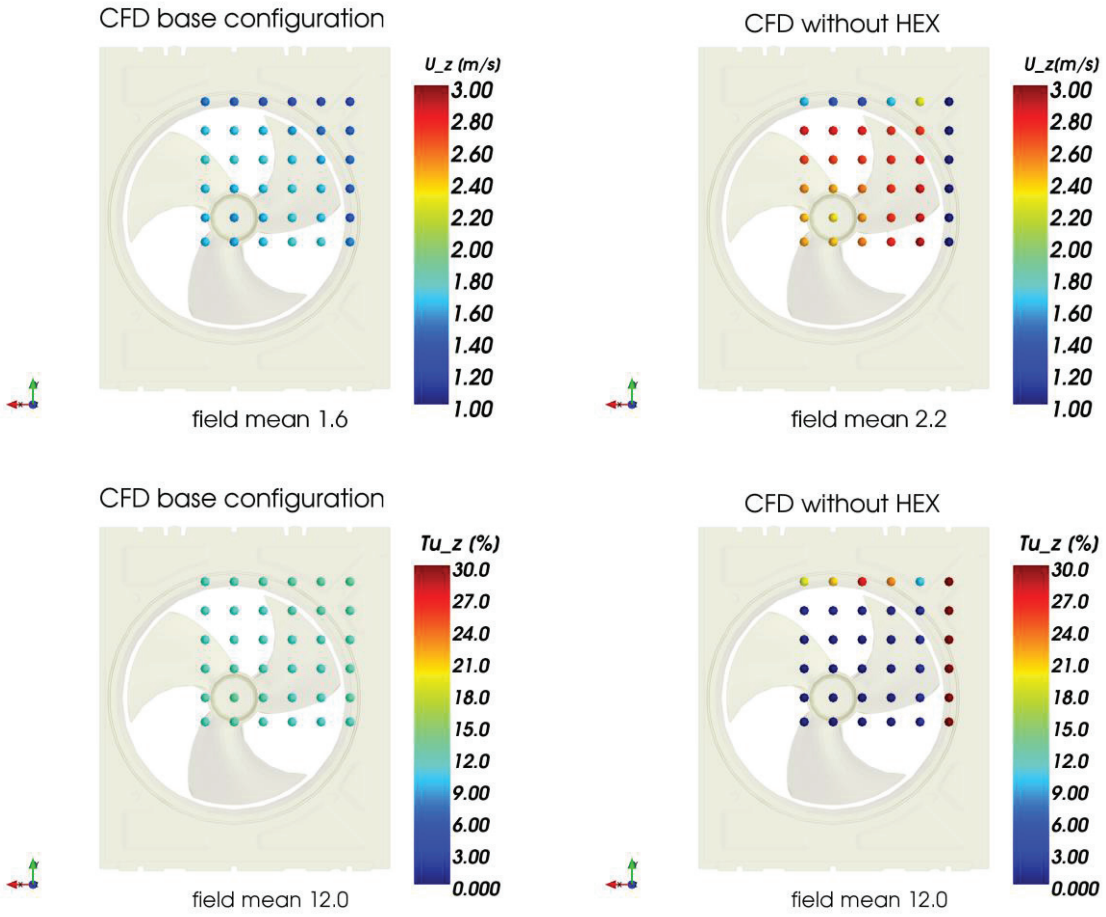

Figure 7. Time averaged URANS results, velocity and turbulence for both configurations

Finally aeroacoustic results are discussed. Figure 8 displays acoustic spectra for both configurations at free blowing conditions. The microphone positions are at 1 m distance to the

appliance on fan axis and 3.4 m off axis respectively. Simulation and experiments are displayed with the same frequency resolution of 5.5 Hz. CAA only provides tonal components at BPF and its harmonics. For tone 1 (33 Hz) the frequency is too low for the acoustic test rig. The correct trend between both configurations is predicted for tones 2 and 3. Configuration 1 shows higher tonal noise, with stronger difference at tone 3. The trend is not correct for tone 4. Tones higher than 5th order are much too low which is attributed to lack of temporal resolution in the simulation. Absolute levels show deviations in the range of 10 dB between measurements and simulations. Even though the simulation time is rather short, CAA results are not expected to improve with longer physical time. Time signals show smooth periodic behavior with very little variation in time.

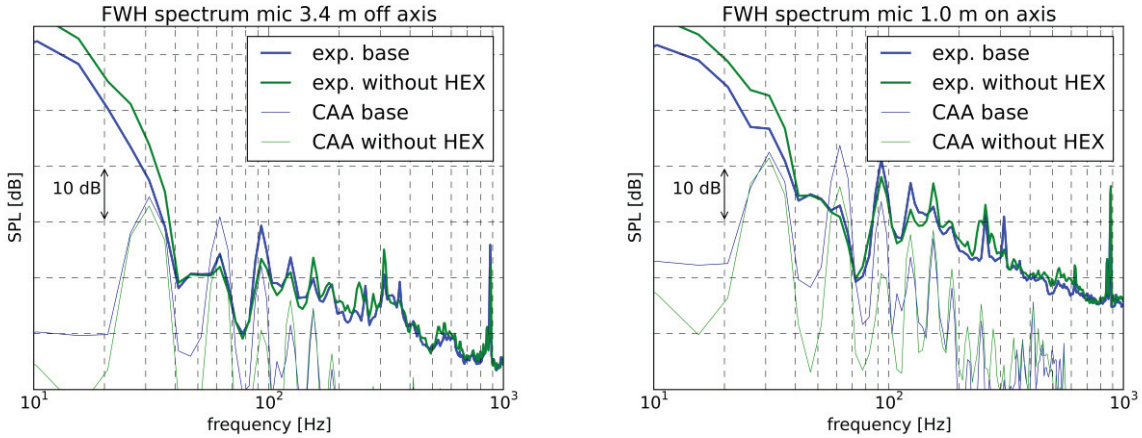

Figure 8. Aeroacoustic simulation results vs. experiments

4. Conclusion

In this paper the effect of heat exchanger in a heat pump on fan noise was investigated. Measurements and simulations show high levels of turbulence in range of 20 % generated by the heat exchanger. Additional turbulence leads to increased fan noise emission of 1 to 2 dB in 3rd octave spectrum. Measured velocity and turbulence are in good agreement with simulations. For the heat exchanger it is important to choose proper boundary conditions to achieve correct turbulence levels. Tuning can be done with auxiliary simulations of detailed heat exchanger geometry. The influence of the heat exchanger on tonal noise was simulated via FW-H based on URANS. The trend between configurations is correctly predicted for most of the tones up to 5th order. The error of absolute levels is up to 10 dB for single tones. For an evaluation of the broad band noise emission turbulence generators are needed as the detailed geometry cannot be resolved in scale resolving simulations. These modelled fluctuations can be used as sources in propagation codes or as transient input for Large Eddy Simulations.

REFERENCES

[1] Carolus T. Ventilatoren, Springer Verlag, 3rd edition, 2013
[2] Zenger F, Renz A, Becher M, Becker S. Experimental investigation of the noise emissions of axial fans under distorted inflow conditions. Journal of Sound and Vibration. 2016, 383:125-145
[3] Rynell A, Efraimsson G, Chevalier M, Abom M. Acoustic characteristics of a heavy duty vehicle cooling module. Applied Acoustics. 2016, 111:67-76
[4] Lucius A, Hütter S, Dietrich P, Schneider M, Lehmann M, Geyer T. Experimental and numerical investigation of axial fan aeroacoustics at disturbed inflow conditions. Proceedings of Fan 2018, Darmstadt
[5] Czwielong F, Krömer F, Becker S. Experimentelle Untersuchung der Schallabstrahlung von Wärmeübertrager-Axialventilator-Modulen. Proceedings of the DAGA 2019, Rostock
[6] Roach PE. The generation of nearly isotropic turbulence by means of grids. Journal of Heat and Fluid Flow. 1987, 8(2):82-92